Nuclear Instruments and Methods in Physics Research B 310 (2013) 81–86

Contents lists available at SciVerse ScienceDirect

Nuclear Instruments and Methods in Physics Research B

journal homepage: www.elsevier.com/locate/nimb

Magnetic and topographical modifications of amorphous Co–Fe thin films induced by high energy Ag^{7+} ion irradiation

G. Pookat [a], T. Hysen [a], S.H. Al-Harthi [b], I.A. Al-Omari [b], R. Lisha [a], D.K. Avasthi [c], M.R. Anantharaman [a,*]

[a] Department of Physics, Cochin University of Science & Technology, Cochin 682022, Kerala, India
[b] Department of Physics, Sultan Qaboos University, Muscat, P.O. Box 36, Code 123, Oman
[c] Inter University Accelerator Centre, Aruna Asaf Ali Marg, New Delhi 110 067, India

ARTICLE INFO

Article history:
Received 23 February 2013
Received in revised form 10 May 2013
Available online 10 June 2013

Keywords:
Co–Fe thin films
SHI irradiation
Structural modification
SRIM simulation
Amorphous structure

ABSTRACT

We have investigated the effects of swift heavy ion irradiation on thermally evaporated 44 nm thick, amorphous $Co_{77}Fe_{23}$ thin films on silicon substrates using 100 MeV Ag^{7+} ions fluences of 1×10^{11} ions/cm^2, 1×10^{12} ions/cm^2, 1×10^{13} ions/cm^2, and 3×10^{13} ions/cm^2. The structural modifications upon swift heavy irradiation were investigated using glancing angle X-ray diffraction. The surface morphological evolution of thin film with irradiation was studied using Atomic Force Microscopy. Power spectral density analysis was used to correlate the roughness variation with structural modifications investigated using X-ray diffraction. Magnetic measurements were carried out using vibrating sample magnetometry and the observed variation in coercivity of the irradiated films is explained on the basis of stress relaxation. Magnetic force microscopy images are subjected to analysis using the scanning probe image processor software. These results are in agreement with the results obtained using vibrating sample magnetometry. The magnetic and structural properties are correlated.

1. Introduction

High magnetic moment Co–Fe alloy films are known for their technological applications such as core material for write elements in modern recording heads and as under-layers in perpendicular media [1–3]. The microstructure of these magnetic thin films plays an important role in determining their magnetic properties, which in turn depends on parameters such as film thickness, crystallinity, surface/interface roughness, and composition. In particular, the variation in surface/interface roughness modifies the magnetic properties such as magnetic anisotropy, coercivity and magnetic domain structure. Thermal annealing [4–5] and swift heavy ion irradiation [6–8] are two effective methods to alter the surface microstructure and morphology. Gupta et al. reported that energy deposition by 120 MeV Au ions leads to changes in structural and magnetic behaviour of Co thin films [9]. Klaumuenzer et al. reported on the plastic deformation of the surface of metallic glasses due to swift heavy ion irradiation [10]. Generally an incident energy equivalent to 1 eV in the sample generates a temperature of $\sim 10^4$ K along the ion trajectory [11]. In ion beam irradiation, the surface topography of the sample is decided by the interplay between the dynamics of surface roughening due to sputtering and smoothing due to material transport during surface diffusion. The competition between these two processes results in the formation of different surface features. Gupta et al. demonstrated that the magnetic field assisted ion implantation is an effective method for the modification of extrinsic magnetic properties of Co–Fe thin films [12]. In short, SHI irradiation can be employed for the topographical modification of surfaces and interfaces in the nanometer scale.

Irradiation results in loss of energy of the ions in the target material via elastic or inelastic collisions. The process through which the swift heavy ions lose their energy can be classified as follows. (i) electronic energy loss $[(dE/dx)_e]$ in which the interaction with target electrons occurs via inelastic collisions which leads to excitation and ionization of target atoms (at energy above $\sim$1 MeV/nucleon), (ii) nuclear energy loss, $[(dE/dx)_n]$ in which direct screened Coulomb interaction with target atom nuclei is responsible for the energy loss and (iii) radiation loss such as Bremsstrahlung and Cerenkov radiation which is very small and can be neglected. The nuclear energy loss is dominant at ion energies below 10 keV/nucleon [13–17]. While irradiating with swift heavy ions, a large amount of energy is transferred to the lattice via electron–phonon interactions. The mechanism behind the energy transfer are well explained using the Coulomb explosion [18,19] and thermal spike model [20–22]. Normally the term 'stopping power' or (dE/dx) is used to describe the energy deposition via the slowing down of ion in the material. However, (dE/dx) gives the energy loss per unit length along the particle trajectory, whereas

* Corresponding author.
E-mail address: mra@gmail.com (M.R. Anantharaman).

0168-583X/$ - see front matter © 2013 Elsevier B.V. All rights reserved.
http://dx.doi.org/10.1016/j.nimb.2013.05.025

the stopping power represents the ability of the material to stop the heavy ions and is represented by $(-1/\delta dE/dx)$, where δ is the density of the material. In swift heavy ion–solid interactions, nuclear stopping power S_n is negligible compared to electronic stopping power S_e. The nuclear interactions result in lattice disorder by the displacement of atoms from their positions whereas, electronic collisions lead to negligible deflection of ion trajectory and small energy loss per interaction. Theoretical calculation of the stopping power can be done using computer simulation methods such as the program TRIM/SRIM (Transport of ions in matter, in more recent versions called Stopping and Range of Ions in Matter). SRIM is a group of programs which calculate the stopping and range of ions in matter using a binary approximation of ion–atom collisions [23]. In such programs the simulation of the ion collisions with nuclei in the medium is carried out to find the stopping power [11].

In this present work, we report on the changes of the topographical and magnetic properties in Ag^{7+} ion irradiated $Co_{77}Fe_{23}$ alloy films. We have chosen Co–Fe thin films for the irradiation studies in light of the fact that the magnetic moment for this alloy is maximum among the 3d ferromagnetic alloys according to the Slater-Pauling curve [24]. Swift heavy ion irradiation effects on the amorphous nature and magnetic texture of amorphous CoFe films have been investigated by MFM/AFM and GXRD studies.

2. Experimental details

Amorphous Co–Fe thin films were deposited by physical vapor deposition technique on naturally oxidized Si (100) substrate. Melt spun ribbon having the composition $Co_{75}Fe_{14}Ni_4Si_5B_2$ was used as the composite target for the deposition. The base pressure in the deposition chamber was maintained at 1×10^{-6} Torr at the time of deposition. The thickness of the prepared films was measured using Dektak 3 thickness profiler as 44 nm. The film samples were mounted on an electrically insulated sample ladder and the ladder current was integrated to collect and count the charge pulses via a scalar counter along with the digital current integrator. 100 MeV Ag^{7+} ions were used to irradiate the Co–Fe films at room temperature with fluences 1×10^{11} ions/cm^2, 1×10^{12} ions/cm^2, 1×10^{13} ions/cm^2, and 3×10^{13} ions/cm^2 using a 15UD Pelletron accelerator at Inter University Accelerator Centre, New Delhi, India. The beam current was maintained at 1.5 pnA (particle nanoampere). This is kept low in order to avoid the heating up of the sample during irradiation. The beam is raster scanned over an area of 1×1 cm^2 using a magnetic scanner. The damage caused by the interaction between the ion beam and target material was calculated using the SRIM software. The electronic stopping power S_e, nuclear stopping power S_n and the residual range R_P of the 100 MeV Ag^{7+} ions in Co–Fe was calculated using SRIM-2006. The typical values of S_e, S_n and R_p are estimated to be 18.16 eV/Å, 2.95×10^3 eV/Å and 6.33 μm, respectively for Ag^{7+} ions having energy 100 MeV in $Co_{77}Fe_{23}$ thin films. The film thickness is much less than the projected range, hence the chances of any ion implantation in the Co–Fe film is very remote. In this experiment the entire contribution of radiation effects due to the passage of ions is by electronic energy loss.

The structural properties of the pristine and irradiated Co–Fe thin films were studied by GXRD (Bruker Discover D-8) with CuK_α (λ = 1.5406 Å) radiation. The surface morphological and magnetic domain patterns were observed using AFM and MFM techniques respectively using AFM multimode instrument, having higher resolution magnetic force microscopy tips (MESP-HR) (Bruker) with resonant frequency of 475 kHz. The MFM is carried out at a scan rate of 0.5 kHz and resolution of 512 pixels. MFM analysis was used to detect the surface magnetisation present in the film via the interaction of the magnetic tip with the stray magnetic field on the sample surface. The quantitative analysis of the AFM images were done with the help of surface analysis software Nanoscope 7.2 (Vecco Scientific Ltd.) to obtain PSD, roughness and depth analysis [25]. The MFM images were analyzed also using SPIP software (version 6.0.6, Image Metrology A/S, Hørsholm, Denmark) to obtain the angular correlation and texture direction index. Room temperature magnetization measurements were carried out using a VSM (DMS 1660 VSM) with a magnetic field varying from −13 to +13 kOe.

3. Results and discussion

The nuclear stopping power, electronic stopping power and projected range were calculated as a function of ion energy using SRIM 2006 and are shown in Fig. 1. The simulation is done for the whole range of energies starting from 0.01 MeV to 10 GeV. Both S_e and S_n increase with increasing energy, reach a maximum value and then start to decrease. The peak in electronic energy loss is known as Bragg peak and the stopping power at energies below the Bragg peak is proportional to the square root of the velocity of ion ($\sim E^{1/2}$). This is given by the LSS theory (Lindhard, Scharff and Schiøtt) [26]. At higher energies above the Bragg peak, the stopping power is proportional to $(1/E)$ and Bethe Bloch relation can be used to corroborate these results [27]. It may be noted that the electronic energy transfer reaches its maximum values at energies higher by many orders than the nuclear stopping power maximum.

The XPS analysis of the as prepared sample confirmed that the films have a nominal composition of $Co_{77}Fe_{23}$ (available as supplementary material). Fig. 2 shows the GXRD patterns corresponding to pristine and irradiated films. The GXRD analysis of the as prepared Co–Fe films shows amorphous nature. The absence of peaks in irradiated Co–Fe films points absence of short range order in the film after irradiation. The energy transfer to the film, with SHI irradiation locally rearranges the atomic structure of the film maintaining the amorphicity of the film. This is clearly visible from the GXRD analysis of the irradiated film.

The surface evolution of the pristine as well as irradiated Co–Fe thin film samples were visible in AFM images shown in Fig. 3(a–e). From the AFM image in Fig. 3(a) it can be inferred that the pristine film surface contains mound-like structures which are considered

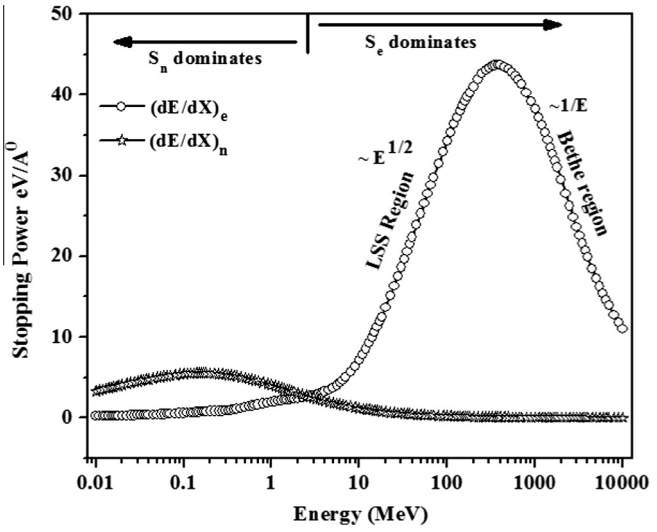

Fig. 1. SRIM simulation for calculating electronic and nuclear energy loss for 100 MeV Ag^{7+} ions in Co–Fe target.

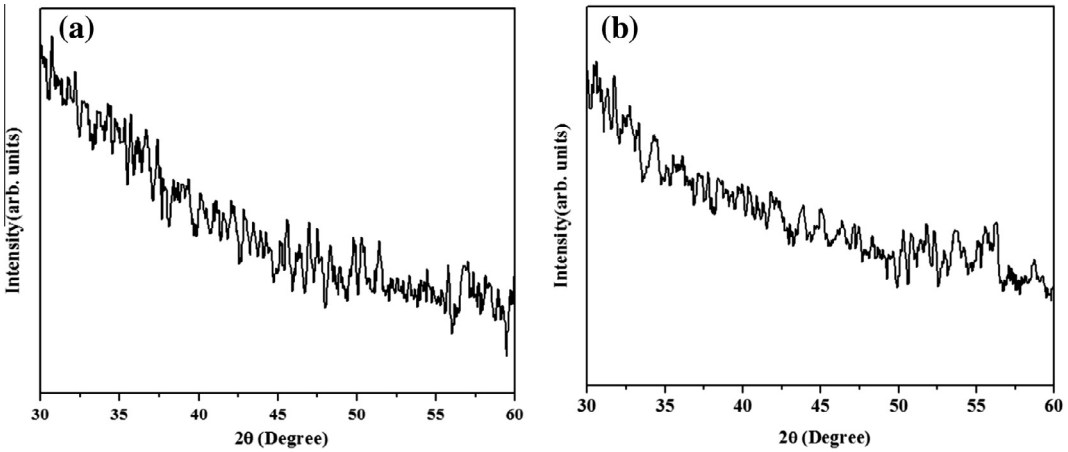

Fig. 2. GXRD of Co–Fe thin film (a) pristine and (b) SHI irradiated at fluence 3×10^{13} ions/cm^2.

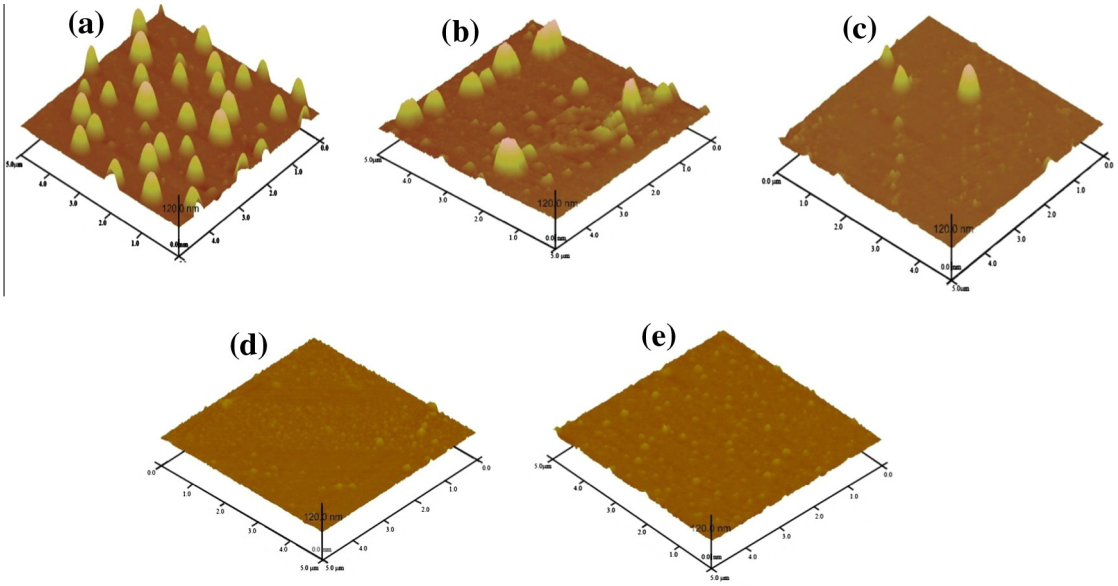

Fig. 3. AFM images of (a) Pristine and Irradiated Co–Fe thin films at fluence (b) 1×10^{11} ions/cm^2 (c) 1×10^{12} ions/cm^2 (d) 1×10^{13} ions/cm^2 (e) 3×10^{13} ions/cm^2.

to be the resultant of the island like growth involved in the vapour deposition process. Fig. 3(b–e) shows the film surface after irradiation at ion fluences 1×10^{11} ions/cm^2, 1×10^{12} ions/cm^2, 1×10^{13} ions/cm^2, and 3×10^{13} ions/cm^2, respectively.

On close analysis of the AFM images it is clear that ion irradiation alters the surface structures found in the pristine sample. The irradiated films show damaged mounds and valleys. No track formation in the ion trajectory is visible in the surface analysis using AFM. As the irradiation dose reaches 3×10^{13} ions/cm^2, the surface show a uniform distribution on all over the scanned area. The root mean square (rms) roughness (R_{rms}) of the films can be calculated using the formula given in Eq. (1) using the standard deviation of the data obtained from AFM images.

$$R_{rms} = \sqrt{\frac{\sum_{n=1}^{N}(Z_n - \bar{z})^2}{N-1}} \quad (1)$$

Here z_n represents the height of the n^{th} data, z is equal to the mean height of z_n in AFM topography, and N is the number of the data points [28]. Dependence of ion fluence on surface roughness of the pristine and SHI irradiated Co–Fe films obtained from AFM images is shown in Fig. 4(a). The rms roughness of the irradiated film follows a rapid decrease followed by further decrease at still higher irradiation dosage like 3×10^{13} ions/cm^2. Surface roughness decreases with ion irradiation indicating the smoothening of the surface upon irradiation. There are many reports on surface smoothing with ion bombardment over a large range of ion energies ~keV to hundreds of MeV [29–34]. Hou et al. in 1990 reported that the electronic excitation and ionization due to irradiation induces rearrangement of atomic ordering and in turn plastic deformation in metallic glasses [35]. Hysen et al. also observed surface smoothing in ion irradiated Fe–Ni thin films [8]. They explained the surface smoothening process at lower fluences using volume diffusion mechanism. At higher fluences they observed surface roughening because of surface evaporation at elevated temperatures. Mayr and Averback also reported similar nature of roughness with irradiation on glassy Zr–Al–Cu films [36] where radiation induced viscous flow was used to explain the dominant surface relaxation mechanism.

Interplay between the dynamics of surface roughening due to sputtering and smoothing due to material transport during surface diffusion plays an important role in the evolution of surface, during ion irradiation [30,37–38]. Information regarding the surface modification mechanisms cannot be completely extracted from the rms

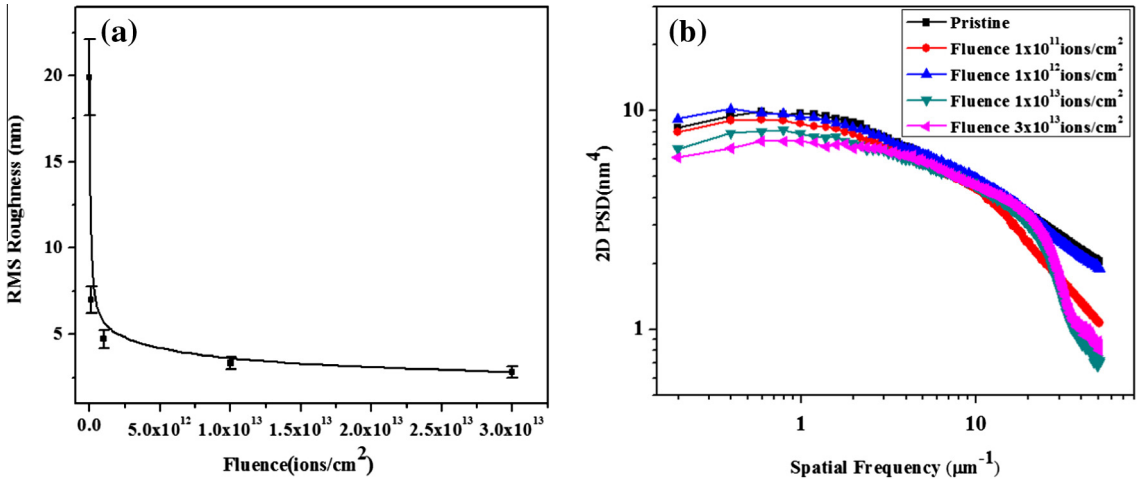

Fig. 4. (a) RMS roughness vs. ion fluence graph and (b) 2D PSD plot of pristine and irradiated films [lines are guide to eye].

surface roughness data, since it measures the roughness in only one direction. PSD analysis is an ideal tool for evaluating the surface roughness both in vertical and horizontal direction and also for determining the dominant process in surface evolution. Fig. 4(b) represents the log–log plots of PSD calculated for pristine and irradiated thin films at various fluences.

The roughness of the pristine film was higher compared to that of irradiated films. In all cases the PSD has two regions, the low frequency part which resembles the uncorrelated white noise and the high frequency part corresponding to the surface evolution. The linear decrease in roughness in the higher frequency region can be modeled using a power law as shown in Eq. (2).

$$\mathrm{PSD}(k) \propto k^{-\gamma} \tag{2}$$

where k represents the spatial frequency, the exponent is the slope of the linear part of the PSD curve which is related to the roughness scaling exponent by the equation $\alpha = (\gamma - d)/2$ [39]. Here the line scan dimension $d = 2$.

According to Herring [40], the values of 1, 2, 3, and 4 represents four modes of surface transport viz. viscous flow, evaporation–condensation, volume diffusion, and surface diffusion, respectively. The values obtained for the irradiated samples are between 0 and 2, hence the dominant surface transport mechanism seems to be a combination of viscous flow and evaporation re-condensation. The dominant surface transport mechanism for the film irradiated at fluence 1×10^{11} ions/cm^2 is irradiation induced viscous flow and that explains the rapid surface smoothening observed at that fluence. As the fluence increases to 1×10^{12} ions/cm^2 and at still higher doses like 1×10^{13} ions/cm^2 and 3×10^{13} ions/cm^2 the dominant mechanism becomes evaporation–condensation due to the sputtering occurring in the film during high energy ion irradiation. The roughness exponent has a value of 1.24, 1.45, 1.29, 1.92, and 1.88, respectively for the as prepared and films irradiated at fluences 1×10^{11} ions/cm^2, 1×10^{12} ions/cm^2, 1×10^{13} ions/cm^2 and 3×10^{13} ions/cm^2. The values of roughness exponent point towards the mechanism of surface evolution [33]. The calculated values of roughness exponent of the pristine and irradiated films clearly explain the surface evolution upon irradiation. Primary smoothening mechanism in the case of crystalline surfaces is found to be surface diffusion whereas that for amorphous surfaces viscous flow dominates [29]. The results obtained from surface roughness analysis are in agreement with the amorphous nature of Co–Fe films concluded from GXRD analysis.

The in-plane hysteresis loops prior to and after irradiation are reported in Fig. 5. Coercivity is decreasing at lower fluence and

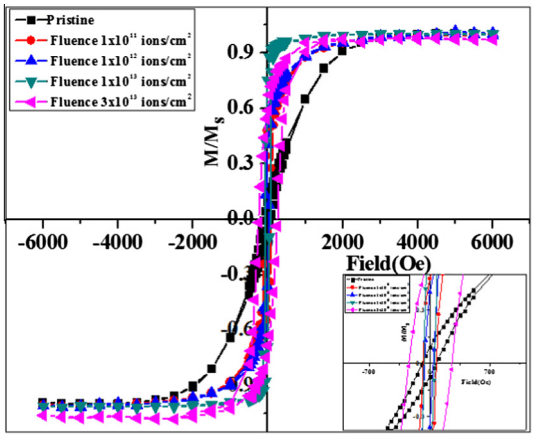

Fig. 5. In plane VSM hysteresis loops for the pristine and SHI irradiated Co–Fe films [inset shows the magnified portion of the centre of hysteresis loop].

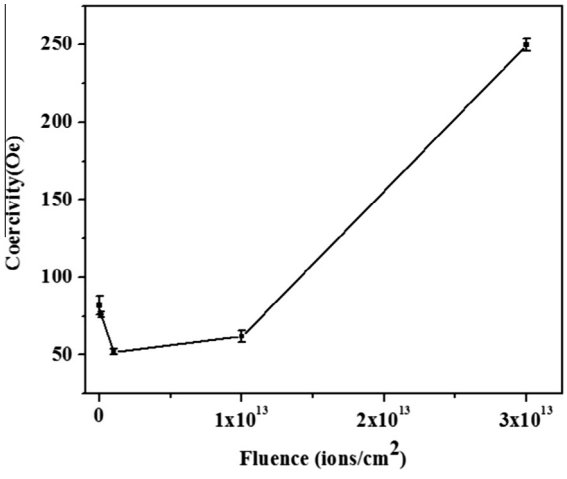

Fig. 6. Variation of coercivity with fluence [lines are guide to eye].

starts to increase at maximum fluence of 3×10^{13} ions/cm^2. It is found that the coercive force of Co–Fe thin films are sensitive to Ag^{7+} ion irradiation and show variation with ion fluence (Fig. 6).

The extrinsic magnetic properties like coercivity and remanence are sensitive to the local structural properties of the films like

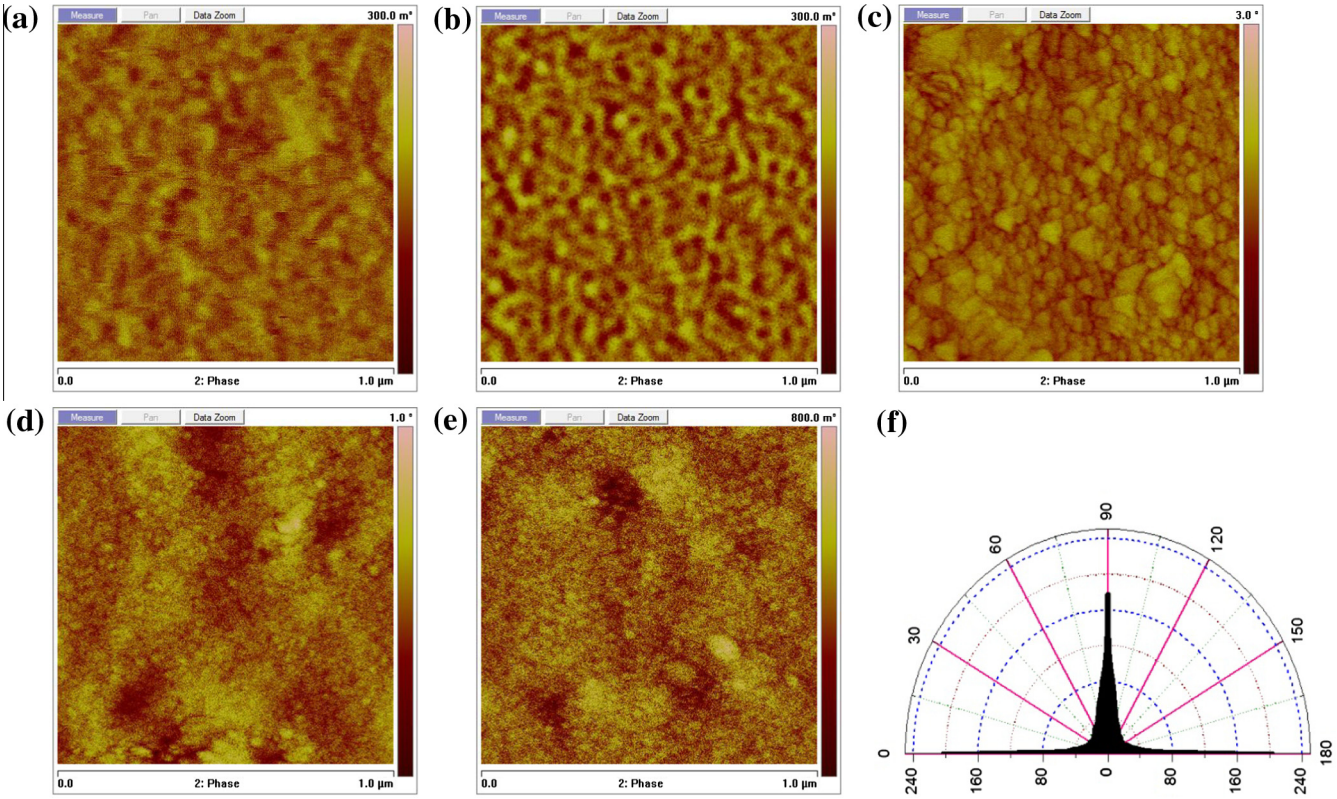

Fig. 7. MFM images of (a) Pristine and SHI irradiated CoFe thin films at fluence (b) 1×10^{11} ions/cm^2 (c) 1×10^{12} ions/cm^2 (d) 1×10^{13} ions/cm^2 (e) 3×10^{13} ions/cm^2 and (f) representative angular spectrum using SPIP software.

strain, grain size, defects etc. The modification of the magnetic properties of the film after irradiation could be explained on the basis of stress and damage induced while irradiation. The coercivity obtained for different fluences decreases at lower fluences up to 1×10^{12} ions/cm^2 and afterwards increases drastically. Ion irradiation results in stress relaxation in the films, which in turn reduces the coercivity at low fluences. The energy transferred to the film during ion irradiation may alter the local atomic arrangement in the amorphous system. Along with this rearrangement there is a chance for increasing the density of the pinning centers for domains at higher fluences which might also be contributing to the observed increase in coercivity.

Fig. 7(a–e) shows the MFM images and corresponding angular spectrum of the pristine and irradiated (at various fluences 1×10^{11} ions/cm^2, 1×10^{12} ions/cm^2, 1×10^{13} ions/cm^2, and 3×10^{13} ions/cm^2) Co–Fe films with scanning size 1 µm × 1 µm. The colour contrast in the images suggests that the magnetisation direction lies out of the plane of the film. Distinctive features of 'dark' and 'bright' stripe magnetic domain structure is observed in the pristine as well as irradiated samples but the contrast and domain pattern is clearly visible in the lowest irradiation dose (1×10^{11} ions/cm^2) compared to others.

By using scanning probe image processor (SPIP) (version 6.0.6) software the angular spectrum of the MFM images and the texture direction index, S_{tdi} were calculated. Texture direction index is defined as the average amplitude sum divided by the amplitude sum of the dominating direction. It is a measure of how well the domains are aligned and the S_{tdi} value is always between 0 and 1. The arrangement of domains can be determined from the value of S_{tdi}. For well aligned domains S_{tdi} values are close to zero, while for a more or less isotropic arrangement, S_{tdi} is close to 1. For the pristine film the measured value of S_{tdi} was 0.202 and for the Ag^{7+} irradiated film, he value is 0.224. This difference reveals that the alignment of the magnetic domains was increased by the Ag-ion irradiation. This again confirms the results obtained from magnetisation analysis.

4. Conclusions

Co–Fe thin films of thickness 44 nm were deposited onto silicon substrates via vacuum evaporation and subjected to SHI irradiation at fluences 1×10^{11} ions/cm^2, 1×10^{12} ions/cm^2, 1×10^{13} ions/cm^2 and 3×10^{13} ions/cm^2. The GXRD results revealed that the amorphous nature of the pristine film is preserved even after irradiation. On SHI irradiation the surface roughness decreases with increase in the irradiation dosage. The roughness exponent of the pristine and irradiated samples calculated from the PSD suggests that the mechanism behind the surface smoothening is viscous flow and evaporation–condensation. The VSM analysis of the pristine and irradiated samples proved that the SHI irradiation of the Co–Fe samples resulted in modifications of magnetic properties. Ion irradiation results in stress relaxation in the films, which in turn reduces the coercivity at low fluences. At a fluence of 3×10^{13} ions/cm^2, the density of the pinning centers increases which results in the observed increase in coercivity. The texture direction index was used to explain the realignment of the magnetic domains upon irradiation. The results obtained from VSM analysis are corroborated with the results obtained using MFM analysis.

Acknowledgment

GP acknowledges UGC, India for providing financial assistance in the form of RFSMS fellowship (No. F4-3/2006(BSR)/8-3/2007(BSR)). H.T. acknowledges financial assistance received from UGC-FDP, India & DST FIST project received by Department of

Physics, Christian College, Chengannur. Kerala, India. LR is thankful to IUAC, New Delhi for providing financial assistance in the form of UFUP project. GP, HT, LR and MRA are thankful to IUAC, New Delhi, India and UGC-DAE Consortium, Indore Centre, Khandwa Road, Indore, India for providing the facility to carry out the experiment. Dr. I. A. Al-Omari would like to thank Sultan Qaboos University for the support under Grant number IG/SCI/PHYS/12/02.MRA acknowledges Department of Science and Technology (DST)-Nano-mission (No. SR/NM/NS-120/2010 (G)) and DST-DAAD (INT/FRG/DAAD/P-207/2011) for providing necessary facilities and financial assistance.

Appendix A. Supplementary data

Supplementary data associated with this article can be found, in the online version, at http://dx.doi.org/10.1016/j.nimb.2013.05.025.

References

[1] T. Osaka, Electrochim. Acta 44 (1999) 3885.
[2] F. Lallemand, D. Comte, L. Ricq, P. Renaux, J. Pagetti, C. Dieppedale, P. Gaud, Appl. Surf. Sci. 225 (2004) 59.
[3] A. Moser, K. Takano, David T. Margulies, Manfred Albrecht, Yoshiaki Sonobe, Yoshihiro Ikeda, Shouheng Sun, E.E. Fullerton, J. Phys. D Appl. Phys. 35 (2002) R157–R167.
[4] D. Aurongzeb, M. Holtz, M. Daugherty, J.M. Berg, A. Chandolu, J. Yun, H. Temkin, Influence of nanocrystal growth kinetics on interface roughness in nickel–aluminum multilayers, Appl. Phys. Lett. 83 (26) (2003) 29.
[5] S. Thomas, S.H. Al-Harthi, D. Sakthikumar, I.A. Al-Omari, R.V. Ramanujan, Y. Yoshida, M.R. Anantharaman, Microstructure and random magnetic anisotropy in Fe–Ni based nanocrystalline thin films, J. Phys. D 41 (2008) 155009.
[6] Y.P. Zhao, R.M. Gamache, G.-C. Wang, T.-M. Lu, G. Palasantzas, J. Hosson, Effect of surface roughness on magnetic domain wall thickness, domain size, and coercivity, J. Appl. Phys. 89 (2001) 1325.
[7] S. Thomas, H. Thomas, D.K. Avasthi, A. Tripathi, R.V. Ramanujan, M.R. Anantharaman, Swift heavy ion induced surface modification for tailoring coercivity in Fe–Ni based amorphous thin films, J. Appl. Phys. 105 (2009) 033910.
[8] Hysen Thomas, Senoy Thomas, Raju V. Ramanujan, D.K. Avasthi, I.A. Al-Omari, Salim Al-Harthi, M.R. Anantharaman, Swift heavy ion induced surface and microstructural evolution in metallic glass thin films, Nucl. Instr. Meth. Phys. Res. B 287 (2012) 85–90.
[9] R. Gupta, A. Khandelwal, D.K. Avasthi, K.G.M. Nair, A. Gupta, Phase transitions in Co thin film induced by low energy and high energy ion beam irradiation, J. Appl. Phys. 107 (2010) 033902.
[10] S. Klaumünzer, Hou Ming-Dong, G. Schumacher, Li Chang-Lin, Ion-beam-induced plastic deformation of amorphous materials, MRS Proceedings, vol. 93, 1987.
[11] D.K. Avasthi, G.K. Mehta, Swift Heavy Ions for Materials Engineering and Nanostructuring, Springer Series in materials science, ISBN 978-94-007-1229-4 (e-book), 2011.
[12] Ratnesh Gupta, G.A. Muller, P. Schaaf, K. Zhang, K.P. Lieb, Magnetic modifications of thin CoFe films induced by Xe+ -ion irradiation, Nucl. Instr. Meth. Phys. Res. B 216 (2004) 350–354.
[13] R.L. Fleischer, P.B. Brice, R.M. Walker, Ion explosion spike mechanism for formation of charged particle tracks in solids, J. Appl. Phys. 36 (1965) 3645.
[14] E. Balanzat, J.C. Jousset, M. Toulemonde, Latent tracks induced by heavy ions in the GeV energy range: results at GANIL, Nucl. Instr. Meth. Phys. Res. B 32 (1988) 368–376.
[15] F. Garrido, A. Benyagoub, A. Chamberod, J.C. Dran, A. Dunlop, S. Klaumunzer, L. Thome Giant, Deformation of solids irradiated with swift heavy ions: behaviour of amorphous/crystalline multilayers, Nucl. Instr. Meth. Phys. Res. B 115 (1996) 430–439.
[16] A. Gupta, D.K. Avasthi, Large electronically mediated sputtering in gold films, Phys. Rev. B 64 (2001) 155407.
[17] S. Kavitha, V. Raghavendra Reddy, Ajay Gupta, D.K. Avasthi, Effect of swift heavy ion irradiation in FePt system, Nucl. Instr. Meth. Phys. Res. 244 (2006) 19–22.
[18] R.L. Fleischer, P.B. Price, R.M. Walker, Ion explosion spike mechanism for formation of charged- particle tracks in solids, J. Appl. Phys. 36 (1965) 3645–3652.
[19] R.L. Fleischer, P.B. Price, R.M. Walker, E.L. Hubbard, Criterion for registration in dielectric track detectors, Phys. Rev. 156 (1967) 353.
[20] A. Iwase, S. Sasaki, T. Iwata, T. Nihira, Anomalous reduction of stage-i recovery in nickel irradiated with heavy ions in the energy range 100–120 MeV, Phys. Rev. Lett. 58 (1987) 2450.
[21] Z.G. Wang, C. Dufour, E. Paumier, M. Toulemonde, The S_e sensitivity of metals under swift-heavy-ion irradiation: a transient thermal process, J. Phys.: Condens. Matter 6 (1994) 6733–6750.
[22] Z.G. Wang, C. Dufour, E. Paumier, M. Toulemonde, The S_e sensitivity of metals under swift-heavy-ion irradiation: a transient thermal process, J. Phys.: Condens. Matter 7 (1995) 2525–2526.
[23] J.F. Ziegler, J.P. Biersack, U. Littmark, The Stopping and Range of Ions in Solids, Pergamon, New York, 1985 (SRIM code: <http://www.srim.org>).
[24] T. Nishizawa, K. Ishida, The Co–Fe (Cobalt–Iron) system, Bull. Alloy Phase Diag. 5 (1984) 250.
[25] E.O. Samy, M.A. Ayman, World Academy of Science, Eng. Technol. 46 (2010).
[26] J. Lindhard, M. Scharff, H.E. Schiott, Range concepts and heavy ion ranges (notes on atomic collisions, II.), Mat. Fys. Medd. Dan. Vid. Selsk. 33 (1963) 14.
[27] F. Bloch, Z. Phys. 81 (1933) 363.
[28] Fuxiang Cheng, Zuoyan Peng, Xu Zhigang, Chunsheng Liao, Chunhua Yan, The sol–gel preparation and AFM study of spinel $CoFe_2O_4$ thin film, Thin Solid Films 339 (1999) 109–113.
[29] E. Chason, T.M. Mayer, B.K. Kellerman, D.T. McIlroy, A.J. Howard, Roughening instability and evolution of the Ge (001) surface during ion sputtering, Phys. Rev. Lett. 72 (1994) 3040.
[30] G. Carter, V. Vishnayakov, Roughening and ripple instabilities on ion-bombarded Si, Phys. Rev. B 54 (1996) 17647.
[31] K. Wittmaack, Practical surface analysis, in: D. Briggs, M.P. Seah (Eds.), Ion and Neutral Spectroscopy, vol. 2, Wiley, Chichester, 1992, p. 122 (Chapter 3).
[32] E.A. Eklund, R. Bruinsma, J. Rudnick, R.S. Williams, Submicron-scale surface roughening induced by ion bombardment, Phys. Rev. Lett. 67 (1991) 1759.
[33] J. Krim, I. Heyvart, D.V. Haesendonck, Y. Bruynseraede, Scanning tunneling microscopy observation of self-affine fractal roughness in ion-bombarded film surfaces, Phys. Rev. Lett. 70 (1993) 57.
[34] A. Gutzmann, S. Klaumunzer, P. Meier, Ion-beam-induced surface instability of glassy $Fe_{40}Ni_{40}B_{20}$, Phys. Rev. Lett. 74 (1995) 2256.
[35] Ming-dong Hou, S. Klaumunzer, G. Schumacher, Dimensional changes of metallic glass during bombardment with fast heavy ions, Phys. Rev. B 41 (1990) 1144.
[36] S.G. Mayr, R.S. Averback, Surface smoothing of rough amorphous films by irradiation-induced viscous flow, Phys. Rev. Lett. 87 (2001) 196106.
[37] S. Jay Chey, J.E. Van Nostrand, D.G. Cahill, Surface morphology of Ge (001) during etching by low-energy ions, Phys. Rev. B 52 (1995) 16696.
[38] D.K. Goswami, B.N. Dev, Nanoscale self-affine surface smoothing by ion bombardment, Phys. Rev. B 68 (2003) 033401.
[39] E.A. Eklund, E.J. Snyder, R.S. Williams, Correlation from randomness: quantitative analysis of ion-etched graphite surfaces using the scanning tunneling microscope, Surf. Sci. 285 (1993) 157.
[40] C. Herring, Effect of change of scale on sintering phenomena, J. Appl. Phys. 21 (1950) 301–303.